



HAL
open science

Thresholds for persistent leaf photochemical damage predict plant drought resilience in a tropical rainforest

Claire Fortunel, Clément Stahl, Sabrina Coste, Camille Ziegler, Géraldine Derroire, Sébastien Levionnois, Isabelle Maréchaux, Damien Bonal, Bruno Hérault, Fabien H Wagner, et al.

► To cite this version:

Claire Fortunel, Clément Stahl, Sabrina Coste, Camille Ziegler, Géraldine Derroire, et al.. Thresholds for persistent leaf photochemical damage predict plant drought resilience in a tropical rainforest. *New Phytologist*, 2023, 239 (2), pp.576-591. 10.1111/nph.18973 . hal-04133784

HAL Id: hal-04133784

<https://hal.inrae.fr/hal-04133784>

Submitted on 20 Jun 2023




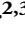














HAL is a multi-disciplinary open access archive for the deposit and dissemination of scientific research documents, whether they are published or not. The documents may come from teaching and research institutions in France or abroad, or from public or private research centers.

L'archive ouverte pluridisciplinaire **HAL**, est destinée au dépôt et à la diffusion de documents scientifiques de niveau recherche, publiés ou non, émanant des établissements d'enseignement et de recherche français ou étrangers, des laboratoires publics ou privés.



Distributed under a Creative Commons Attribution 4.0 International License

Thresholds for persistent leaf photochemical damage predict plant drought resilience in a tropical rainforest

Claire Fortunel¹ , Clément Stahl² , Sabrina Coste² , Camille Ziegler^{2,3} , Géraldine Derroire⁴ ,
Sébastien Levionnois^{1,2} , Isabelle Maréchaux¹ , Damien Bonal³ , Bruno Hérault^{5,6,7} ,
Fabien H. Wagner^{8,9} , Lawren Sack¹⁰ , Jérôme Chave¹¹ , Patrick Heuret¹ , Steven Jansen¹² ,
Grace John¹³ , Christine Scoffoni¹⁴ , Santiago Trueba¹⁵  and Megan K. Bartlett¹⁶ 

¹AMAP (Botanique et Modélisation de l'Architecture des Plantes et des Végétations), Université de Montpellier, CIRAD, CNRS, INRAE, IRD, 34000 Montpellier, France; ²INRAE, UMR EcoFoG, CNRS, CIRAD, AgroParisTech, Université des Antilles, Université de Guyane, 97310 Kourou, France; ³Université de Lorraine, AgroParisTech, INRAE, UMR Silva, 54000 Nancy, France; ⁴CIRAD, UMR EcoFoG (AgroParisTech, CNRS, INRAE, Université des Antilles, Université de la Guyane), Campus Agronomique 97310 Kourou, French Guiana; ⁵CIRAD, UPR Forêts et Sociétés, Yamoussoukro, Côte d'Ivoire; ⁶Forêts et Sociétés, Univ Montpellier, CIRAD, 34000 Montpellier, France; ⁷Institut National Polytechnique Félix Houphouët-Boigny, INP-HB, Yamoussoukro, Côte d'Ivoire; ⁸Institute of Environment and Sustainability, University of California, Los Angeles, CA 90095, USA; ⁹Jet Propulsion Laboratory, California Institute of Technology, 4800 Oak Grove, Pasadena, CA 91109, USA; ¹⁰Department of Ecology and Evolutionary Biology, University of California, Los Angeles, CA 90095, USA; ¹¹CNRS, Université Toulouse 3 Paul Sabatier, IRD, UMR 5174 Evolution et Diversité Biologique (EDB), 31062 Toulouse, France; ¹²Institute of Botany, Ulm University, Albert-Einstein-Allee 11, 89081 Ulm, Germany; ¹³Department of Biology, University of Florida, Gainesville, FL 32611, USA; ¹⁴Department of Biological Sciences, California State University, Los Angeles, CA 90032, USA; ¹⁵Université de Bordeaux, INRAE, UMR BIOGECO, Pessac 33615, France; ¹⁶Department of Viticulture and Enology, University of California, Davis, CA 95616, USA

Summary

Author for correspondence:
Megan K. Bartlett
Email: mkbartlett@ucdavis.edu

Received: 13 January 2023
Accepted: 12 April 2023

New Phytologist (2023) **239**: 576–591
doi: 10.1111/nph.18973

Key words: drought, embolism resistance, hydraulics, photochemistry, recovery, rehydration, tropical.

- Water stress can cause declines in plant function that persist after rehydration. Recent work has defined 'resilience' traits characterizing leaf resistance to persistent damage from drought, but whether these traits predict resilience in whole-plant function is unknown. It is also unknown whether the coordination between resilience and 'resistance' – the ability to maintain function during drought – observed globally occurs within ecosystems.
- For eight rainforest species, we dehydrated and subsequently rehydrated leaves, and measured water stress thresholds for declines in rehydration capacity and maximum quantum yield of photosystem II (F_v/F_m). We tested correlations with embolism resistance and dry season water potentials (Ψ_{MD}), and calculated safety margins for damage (Ψ_{MD} – thresholds) and tested correlations with drought resilience in sap flow and growth.
- Ψ thresholds for persistent declines in F_v/F_m , indicating resilience, were positively correlated with Ψ_{MD} and thresholds for leaf vein embolism. Safety margins for persistent declines in F_v/F_m , but not rehydration capacity, were positively correlated with drought resilience in sap flow.
- Correlations between resistance and resilience suggest that species' differences in performance during drought are perpetuated after drought, potentially accelerating shifts in forest composition. Resilience to photochemical damage emerged as a promising functional trait to characterize whole-plant drought resilience.

Introduction

Water stress not only impairs plant function during drought but can also irreversibly damage hydraulic and photosynthetic tissues (Buckley *et al.*, 1980), inducing declines in gas exchange and growth that persist after drought (Anderegg *et al.*, 2015; Skelton *et al.*, 2017). As drought intensity and frequency increase under climate change in many regions world-wide (Yuan *et al.*, 2019), limited recovery from water stress could become an increasingly important constraint on plant performance and ecosystem carbon

uptake. Thus, characterizing plant drought resilience – the capacity to experience drought without sustaining lasting damage – has strong potential to improve predictions for ecosystem responses to climate change. Resilience captures adaptation to drought more broadly than classic drought resistance – the ability to maintain function during drought – by also incorporating the capacity to recover function after drought, in response to rehydration (Fletcher *et al.*, 2022). Here, we characterized drought resilience in leaf function in eight tropical tree species and tested for the first time how these traits are associated with the complex

of drought resistance traits and with whole-plant drought resilience in a natural ecosystem.

Persistent damage to leaf hydraulics or photochemistry can constrain plant gas exchange and growth after drought by impairing leaf function and reducing effective canopy size. Drought-induced embolism formation in the veins (Johnson *et al.*, 2018) and structural damage to cell walls and membranes in the mesophyll (Trifilò *et al.*, 2021) can cause persistent declines in leaf hydraulic conductance (K_{leaf}), limiting the water supply for transpiration and, consequently, stomatal reopening. Severely droughted plants (i.e. to an 80–95% reduction in K_{leaf}) typically fail to fully recover to well-watered values for K_{leaf} and stomatal conductance after days or even weeks of rehydration (Skelton *et al.*, 2017; Johnson *et al.*, 2018; but see Manzi *et al.*, 2022), whereas these functions usually fully recover with overnight rehydration in plants subjected to milder water stress (Blackman *et al.*, 2009). Drought can also limit recovery in photosynthesis by deforming the thylakoid membranes and exacerbating reactive oxygen species attacks on the electron transport chain (Miller *et al.*, 2010; Abid *et al.*, 2016), which can cause persistent declines in the effective and maximum quantum yield of photosystem II (PSII) by impairing the electron donor function in PSII and reducing connectivity and energy transport between PSII units (Souza *et al.*, 2004; Campos *et al.*, 2014; Silva *et al.*, 2015). Photochemical function can also continue to decline despite rehydration, as re-expansion further damages membranes that were deformed by drought, or drought triggers leaf senescence and initiates a program of chloroplast and cell death that is not reversed by rehydration (Kaiser, 1987; Munné-Bosch *et al.*, 2001; Brodribb *et al.*, 2021). Beyond these effects on leaf-level gas exchange, inducing leaf senescence and reducing effective canopy size can also cause persistent declines in whole-plant gas exchange, which can, in turn, limit the carbon available for growth (Brodribb *et al.*, 2010; Anderegg *et al.*, 2014). Stem diameter growth can also remain limited after drought despite full recovery in carbon assimilation, due to lagged recovery in respiratory processes (Saveyn *et al.*, 2007) or significant carbon allocation to repairing or replacing damaged tissues or replenishing carbohydrate reserves (Kannenberg *et al.*, 2019).

These findings suggest that traits measuring resilience in leaf function to persistent damage from drought could be used to characterize resilience in whole-plant function, analogous to the use of drought resistance traits to infer whole-plant hydraulic function and gas exchange during water stress (Buckley *et al.*, 1980; Sterck *et al.*, 2011; Maréchaux *et al.*, 2018; Trueba *et al.*, 2019). Two traits have been proposed to capture drought resilience in leaf water relations and photochemical function: the water stress thresholds inducing declines in the rehydration capacity and maximum quantum yield of photosystem II (F_v/F_m) in droughted and rehydrated leaves, relative to unstressed (saturated) leaves (Oppenheimer & Leshem, 1966; John *et al.*, 2018; Trueba *et al.*, 2019; Fig. 1). The relative water content (RWC) or water potential (Ψ) during dehydration defines the threshold for the percent loss of rehydration capacity (PLRC) and percent loss of chlorophyll fluorescence (PLCF) in rehydrated compared with saturated leaves (Trueba *et al.*, 2019; Table 1; Fig. 1). For

example, $\Psi@PLRC_{10}$ measures the water potential during dehydration that induces leaves to rehydrate to a relative water content value 10% lower than when unstressed (saturated), and $\Psi@PLCF_{10}$ measures the dehydrated water potential inducing a 10% reduction in F_v/F_m in rehydrated, compared with unstressed, leaves. $\Psi@PLCF$ captures the water stress thresholds for persistent biochemical limitations on photosynthesis, including damage to thylakoid membrane structure and chloroplast and cell death (Campos *et al.*, 2014; Abid *et al.*, 2016; Guadagno *et al.*, 2017; Fig. 1). $\Psi@PLRC$ captures thresholds for a broad range of hydraulic damage, since rehydration capacity can be limited by reduced water inflow, due to embolism or damage to the extraxylary pathway (Johnson *et al.*, 2018), and/or by a diminished capacity to hold water in the mesophyll, due to cell death or membrane damage that prevents the cells from fully reinflating (Sancho-Knapik *et al.*, 2011; Trifilò *et al.*, 2021; Fig. 1). However, $\Psi@PLRC$ and $\Psi@PLCF$ thresholds have not been tested for their capacity to predict resilience in gas exchange and growth in intact whole plants, or compared with plant water stress *in situ* to evaluate how frequently plants experience persistent damage in natural ecosystems.

Drought resilience is a product of both resistance and recovery, but the relative importance of resistance and recovery to resilience is poorly understood, despite potentially significant effects on ecosystem drought responses. Climate change is expected to intensify drought in many areas, and a strong coordination between drought resilience and resistance would indicate that species differences in performance during drought would propagate into subsequent wet periods, potentially exacerbating drought-induced shifts in community composition and diversity (Flynn *et al.*, 2011). Alternatively, a stronger relationship between resilience and recovery could allow a strong recovery in performance after drought to compensate for greater damage and poorer performance during drought, counteracting drought impacts on species performance differences (Forner *et al.*, 2014; Ploughe *et al.*, 2019). In previous work, RWC and $\Psi@PLRC_{10}$ were correlated with leaf drought resistance traits, including resistance to wilting and declines in hydraulic conductivity under water stress, across species from biomes that varied widely in water availability (i.e. from semideserts to tropical forests; John *et al.*, 2018; Trueba *et al.*, 2019). However, if these correlations result from independent selection by water availability, these traits could be decoupled across species from the same ecosystem, which generally occupy a narrower range of climatic conditions. Indeed, this is the case for leaf drought resistance and economics spectrum traits (e.g. leaf mass per area), which are in some cases correlated across species from different ecosystems, but decoupled across co-occurring species from tropical rainforests (Zhu *et al.*, 2018; Maréchaux *et al.*, 2020).

We measured the water potential thresholds for persistent declines in leaf rehydration capacity and photochemical function for eight tropical species that were also assessed for drought resistance traits, water stress (i.e. dry season midday water potentials, Ψ_{MD}), and drought resilience in whole-plant sap flow and stem diameter growth (Fig. 2). We focused on tropical species because, across a global comparison, these species were the most

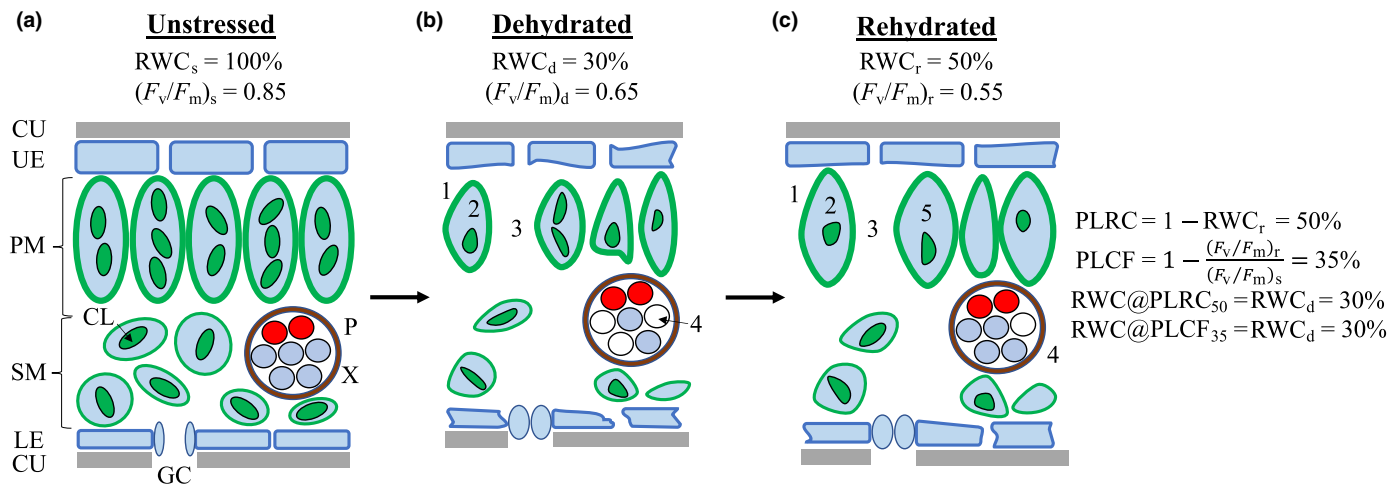


Fig. 1 Water stress induces damage that prevents rehydrated leaves from fully recovering hydraulic and photochemical function. Each panel shows a leaf cross-section. CU, cuticle; UE, upper epidermis; PM, palisade mesophyll; CL, chloroplasts; SM, spongy mesophyll; LE, lower epidermis; GC, guard cells; P, phloem (red circles); X, xylem (blue circles indicate water-filled and white circles indicate embolized conduits); RWC, leaf relative water content; F_v/F_m , maximum quantum yield of photosystem II. Values for saturated, dehydrated, and rehydrated leaves are indicated with subscripts s, d, and r, respectively. (a) F_v/F_m and RWC are at maximum in the saturated, unstressed leaf. (b) Severely dehydrating the leaf can deform cell walls and chloroplast thylakoid membranes (1), trigger chloroplast degradation and cell death (2, 3), and embolize xylem conduits (4) (Oppenheimer & Leshem, 1966; Sancho-Knapik *et al.*, 2011; Johnson *et al.*, 2018; Trifilò *et al.*, 2021). Numbers indicate examples in the cross-section. (c) Negligible or partial xylem embolism refilling (4), cell death (3), and cell wall deformation (1) can prevent the leaf from fully rehydrating (Oppenheimer & Leshem, 1966; Johnson *et al.*, 2018). Recovery in F_v/F_m can be limited by chloroplast degradation (2) and cell death (3) during dehydration (Munné-Bosch *et al.*, 2001). F_v/F_m can also continue to decline despite rehydration because re-expansion further damages the deformed thylakoid membranes, or because drought triggers leaf senescence and initiates a program of chloroplast (5) and cell death that is not reversed by rehydration (Kaiser, 1987; Munné-Bosch *et al.*, 2001; Brodribb *et al.*, 2021). The leaf drought resilience traits measure the dehydration thresholds for declines in function that persist after rehydration. Here, dehydrating leaves (b) to 30% of the saturated water content (RWC_d = 30%) induced a 50% loss of rehydration capacity (PLRC₅₀) and 35% loss of chlorophyll fluorescence (PLCF₃₅) in rehydrated, compared with saturated, leaves, defining the dehydration thresholds RWC@PLRC₅₀ = RWC@PLCF₃₅ = 30%.

vulnerable to persistent damage (John *et al.*, 2018), and severe drought causes persistent reductions in the tropical carbon sink (Yang *et al.*, 2018). We evaluated the coordination between drought resilience and resistance by testing correlations between the thresholds for persistent damage, leaf and stem embolism resistance, and dry season water potentials. We hypothesized that plants would adapt to undergo more negative water potentials in the dry season by increasing both resistance to damage during drought and resilience to persistent damage after drought (Fig. 2, #1–7). We assessed species' risk of damage during and after drought by calculating hydraulic safety margins, as the differences between Ψ_{MD} and the thresholds inducing embolism and persistent damage to rehydration capacity and photochemical function. We hypothesized that smaller safety margins predict larger persistent declines in sap flow and stem diameter growth (Fig. 2, #8–13). Persistent damage to leaf function or drought-induced leaf senescence could cause persistent reductions in canopy-scale transpiration and carbon assimilation, thereby reducing plant sap flow and stem growth.

Materials and Methods

Study site and species

This study was conducted at the Paracou long-term research station in French Guiana (5°16'26"N, 52°55'26"W), a lowland tropical forest, with a mean annual temperature of 25.7°C and annual precipitation of 3102 mm (Gourlet-Fleury *et al.*, 2004).

Precipitation is seasonal, with nearly two-thirds of annual rainfall occurring from March to June. Paracou experiences an annual dry season from mid-August to mid-November, with < 100 mm of rainfall per month (Aguilos *et al.*, 2019). The site is highly diverse, with > 546 woody species with DBH ≥ 2 cm reported within 5 ha (Molino & Sabatier, 2001).

We selected eight abundant tree species that had previously been measured for leaf and stem hydraulic traits and dry season water potentials to measure here for leaf drought resilience (Table 2). Half of the species are evergreen, one is drought-deciduous, and three are supra-annually deciduous and undergo leaf turnover after multiple years in almost any month (Loubry, 1994). We selected canopy (*c.* 50 m) trees with a DBH ≥ 10 cm and direct illumination on ≥ 50% of the canopy area from the Gyaflux eddy covariance tower footprint (see Table 2 for sample sizes). We worked with tree climbers to sample 2–3 m sunlit branches early in the dry season (i.e. early to mid-September 2019). Sampled branches were kept in humidified bags, with the cut ends wrapped in wet paper towels, and transported to the laboratory in the afternoon. Branches were then recut underwater two nodes above the initial cut and rehydrated overnight inside humidified bags under cool, dark conditions.

Measuring thresholds for persistent declines in leaf rehydration capacity and photochemical function

We characterized the water stress thresholds for persistent declines in leaf rehydration capacity and chlorophyll fluorescence

Table 1 Key symbols and definitions.

Symbol	Units	Definition
Water status and photochemical function		
RWC _d	%	Dehydrated leaf relative water content
F _v /F _m	–	Maximum quantum yield of photosystem II
PLRC	%	Percent loss of rehydration capacity, the difference in relative water content between saturated and rehydrated leaves
PLCF	%	Percent loss of chlorophyll fluorescence, the percent decline in F _v /F _m in rehydrated compared with saturated leaves
Leaf resilience traits		
Ψ@PLRC ₃₅ , Ψ@PLRC ₅₀	MPa	Dehydrated water potential (Ψ) threshold inducing a 35% (or 50%) decline in relative water content in rehydrated, compared with unstressed, leaves (i.e. a 35% or 50% loss of rehydration capacity)
Ψ@PLCF ₃₅ , Ψ@PLCF ₅₀	MPa	Dehydrated Ψ threshold inducing a 35% (or 50%) loss of chlorophyll fluorescence in rehydrated, compared with unstressed, leaves
Drought resistance traits		
LXE Ψ ₁₂ , Ψ ₅₀ , Ψ ₈₈	MPa	Leaf water potential inducing 12%, 50%, or 88% embolism spread in the leaf xylem
K _{stem} Ψ ₁₂ , Ψ ₅₀ , Ψ ₈₈	MPa	Stem water potential inducing a 12%, 50%, or 88% decline in stem hydraulic conductivity, respectively
Ψ _{MD}	MPa	Dry season midday leaf water potential
Plant sapflow resilience		
PET	mm d ⁻¹	Cumulative daily potential evapotranspiration
D _s	kg dm ⁻² d ⁻¹	Cumulative daily tree sapflux density
Δ _{sapflow}	%	Percent change in D _s in the postdrought compared with predrought period, calculated at the mean PET (i.e. 7.5 mm d ⁻¹)
Stem growth resilience		
β _s	–	Modeled effect of the intensity of the preceding dry season on the wet season diameter growth rate for each species (s)

using the methods of Trueba *et al.* (2019). Eight to 16 mature, fully expanded leaves were sampled from each rehydrated branch (*n* = 37–58 per species; Table 2, Supporting Information Table S1). All leaves were excised at the same time each morning, to ensure a consistent rehydration time, then double-bagged, and kept humid by placing wet paper towels in the outer bags. Leaves were weighed for saturated mass (*M*_s), then dark-adapted for 30 min, and measured for chlorophyll fluorescence with a MINI-PAM II pulse-modulated fluorometer (Walz, Effeltrich, Germany). Leaves were measured for minimum fluorescence (*F*₀), then exposed to a saturating pulse of red light (650 nm) at 5000 μmol m⁻² s⁻¹ for 0.8 s, and measured for maximum fluorescence (*F*_m). These measurements were used to calculate *F*_v/*F*_m, the maximum quantum yield of photosystem II, as:

$$\frac{F_v}{F_m} = \frac{F_m - F_o}{F_m} \quad \text{Eqn 1}$$

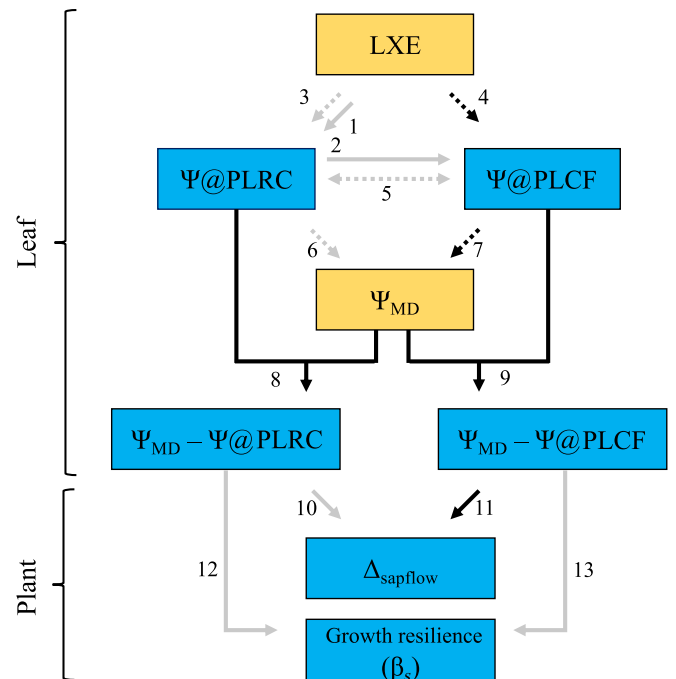


Fig. 2 Hypothesized and observed correlations with the leaf drought resilience traits. Solid lines show causative, and dashed lines show correlative relationships. Black lines indicate statistically significant correlations. Box fill color indicates drought resilience (blue) or drought resistance (gold) traits. Brackets indicate variables were measured at the leaf or plant scale. (1, 2) We hypothesized that leaf xylem embolism could prevent leaves from rehydrating and, thus, recovering photochemical function, driving causative relationships between water potential thresholds for leaf embolism resistance (LXE), loss of rehydration capacity (Ψ@PLRC), and loss of chlorophyll fluorescence (Ψ@PLCF; Brodribb *et al.*, 2021; Trifilò *et al.*, 2021). (3–5) Alternatively, these traits could be correlated, but not causatively related, if leaves have evolved to stop repairing damage and initiate senescence as the veins embolize, to avoid wasting resources on repairing a hydraulically compromised leaf (Munné-Bosch *et al.*, 2001). On the contrary, recent work has hypothesized that water storage and photosynthesis are specialized on different tissues (i.e. the spongy and palisade mesophyll, respectively), which could allow Ψ@PLRC and Ψ@PLCF to vary independently (Xiong & Nadal, 2020). (6, 7) We hypothesized leaves would regulate water potential to avoid persistent damage, producing correlations between the damage thresholds and midday water potentials in the dry season (Ψ_{MD}). (8, 9) The difference between these thresholds and Ψ_{MD} defines the safety margins for persistent damage. (10, 11) Plants with smaller safety margins would be more vulnerable to persistent leaf damage, which we hypothesized would limit leaf-level gas exchange and/or reduce canopy area by triggering the senescence of damaged leaves, thereby reducing canopy-level gas exchange and, consequently, sap flow (Blackman *et al.*, 2009). We measured drought resilience in sap flow as Δ_{sapflow}, the percent change in cumulative daily sapflux before and after the 2018 dry season. (12, 13) We hypothesized that persistent reductions in leaf function would limit plant carbon assimilation and, consequently, stem diameter growth (Brodribb *et al.*, 2010; Kannenberg *et al.*, 2019). We quantified drought resilience in growth by fitting β_s, the slope of the relationship between the intensity of the dry season and stem growth rate in the subsequent wet season. Greater resilience to photochemical damage was significantly correlated with greater resilience to leaf xylem embolism and more negative water potentials in the dry season (Table 5; Fig. 4a,c). Larger safety margins for persistent photochemical damage were significantly correlated with greater drought resilience in whole-plant sap flow (Table 6; Fig. 7).

Table 2 Leaf water potential thresholds inducing 35% and 50% declines in rehydration capacity (i.e. $\Psi@PLRC_{35}$ and $\Psi@PLRC_{50}$) and photochemical function (i.e. $\Psi@PLCF_{35}$ and $\Psi@PLCF_{50}$) in rehydrated, compared with unstressed, leaves of eight rainforest species.

Species	Family	Phenology	$\Psi@PLRC_{35} \pm SD$ (MPa)	$\Psi@PLRC_{50} \pm SD$ (MPa)	n_{leaf}	$\Psi@PLCF_{35} \pm SD$ (MPa)	$\Psi@PLCF_{50} \pm SD$ (MPa)	n_{leaf}	n_{indiv}
<i>Bocoa prouacensis</i> (Aubl.)	Fabaceae	E?	-1.83 ± 0.26	-2.69 ± 0.41	57	-3.10 ± 0.58	-4.90 ± 0.78	59	4
<i>Dicorynia guianensis</i> (Amshoff)	Fabaceae	D	-1.80 ± 0.28	-2.39 ± 0.38	45	-1.91 ± 0.32	-2.17 ± 0.33	48	3
<i>Eperua falcata</i> (Aubl.)	Fabaceae	D	-1.94 ± 0.25	-2.53 ± 0.34	38	-2.46 ± 0.35	-2.88 ± 0.35	39	3
<i>Eperua grandiflora</i> (Aubl.)	Fabaceae	E?	-2.13 ± 0.32	-2.79 ± 0.45	36	-2.42 ± 0.68	-3.67 ± 0.60	36	3
<i>Eschweilera sagotiana</i> (Miers)	Lecythidaceae	E?	-1.88 ± 0.24	-2.54 ± 0.33	40	-1.58 ± 0.20	-1.80 ± 0.20	47	3
<i>Lecythis poiteaui</i> (O. Berg)	Lecythidaceae	D	-2.23 ± 0.35	-2.78 ± 0.45	43	-2.96 ± 0.57	-3.36 ± 0.58	46	3
<i>Pradosia cochlearia</i> ((Lecomte) T.D. Penn.)	Sapotaceae	DD	-2.35 ± 0.34	-2.92 ± 0.53	45	-2.92 ± 0.53	-3.47 ± 0.59	45	3
<i>Virola michelii</i> (Heckel)	Myristicaceae	E	-1.98 ± 0.23	-2.32 ± 0.30	38	-2.13 ± 0.33	-2.87 ± 0.30	46	3

n_{indiv} is the number of individuals and n_{leaf} is the number of leaves sampled per species for each trait. Leaves were pooled to calculate one value of each threshold per species. SD is the standard deviation, calculated by propagating uncertainty from the leaf osmotic potential measurements and best-fit relationships between leaf dehydration, PLRC, and PLCF (see Supporting Information Methods S1). Best-fit relationships are shown in Figs S1 and S2. Names in parentheses following the species binomials indicate taxonomic authorities. Phenological categories are E for evergreen, DD for drought-deciduous (i.e. with leaf-fall concentrated in the September–November dry season), and D for nondrought-deciduous (i.e. with leaf-fall occurring throughout the year; Ziegler *et al.*, 2019). Question marks indicate these classifications are based on observations by site botanists but have not been confirmed with litterfall monitoring. Thresholds measured in units of relative water content (e.g. $RWC@PLRC_{35}$) are provided in Table S3. Standard deviations for the RWC thresholds are provided in Table S4.

Leaves were then bench-dehydrated under ambient laboratory conditions. Each leaf was measured once for dehydrated mass (M_d) and dehydrated F_v/F_m . Dehydration times were varied across leaves to generate a wide range in water stress for each species. Measured leaves were then double-bagged to avoid water loss until all leaves could be arranged for rehydration at the same time each night. To rehydrate, the petioles were submerged in water, while avoiding wetting the blade, and the leaves were covered with humidified bags. Leaves were rehydrated overnight (12 h), all rebagged at the same time the next morning and measured for rehydrated mass (M_r) and rehydrated F_v/F_m . Leaves were then oven-dried at 70°C for 72 h to measure dry mass (M_{dry}).

Dehydrated and rehydrated leaf relative water contents (RWC_d and RWC_r) were calculated as:

$$RWC_d = \frac{M_d - M_{dry}}{M_s - M_{dry}} \quad \text{Eqn 2a}$$

$$RWC_r = \frac{M_r - M_{dry}}{M_s - M_{dry}} \quad \text{Eqn 2b}$$

and the percent loss of relative water content and F_v/F_m between saturated (s) and rehydrated (r) leaves (PLRC and PLCF) were calculated as:

$$PLRC = 100(1 - RWC_r) \quad \text{Eqn 3a}$$

$$PLCF = 100 \left(1 - \frac{(F_v/F_m)_r}{(F_v/F_m)_s} \right) \quad \text{Eqn 3b}$$

where PLRC or PLCF = 0 indicates the rehydrated leaves fully recovered to saturated values.

Damage thresholds were calculated by using maximum likelihood to fit relationships between PLRC or PLCF (y) as functions

of water stress ($x = RWC_d$). We pooled all leaves for each species, and, since the shape of these relationships can vary across species (Trueba *et al.*, 2019), fitted each species with linear ($y = a + bx$), exponential ($y = ae^{-bx}$), and sigmoidal ($y = a/(1 + e^{-(x-c)/b})$) functions using the LIKELIHOOD package in R (v.4.1.0; Murphy, 2015; Table S2; Figs S1, S2). We selected the best-fit model for each species, as either the model with the lowest AICc value (Akaike Information Criterion corrected for small sample sizes), if that value was ≥ 2 units below the other models, or the most parsimonious model with an AICc value within 2 units of the lowest AICc (Burnham & Anderson, 2010). Best-fit relationships were mostly linear for PLRC (i.e. 5/8 species) and sigmoidal for PLCF (i.e. 6/8 species; Table S2; Figs S1, S2). The best-fit model for each species was used to calculate the RWC_d values inducing 35% and 50% declines in RWC and F_v/F_m in rehydrated compared with saturated leaves (i.e. $RWC@PLRC_{35}$, $RWC@PLRC_{50}$, $RWC@PLCF_{35}$, and $RWC@PLCF_{50}$; see the explanation for these thresholds below).

The RWC_d thresholds were converted to water potentials (Ψ) with the pressure–volume curve equation:

$$\Psi = \frac{\pi_o (1 - a_f)}{(RWC/100 - a_f)} \quad \text{for } \Psi \leq \pi_{tlp} \quad \text{Eqn 4}$$

where π_o is the osmotic potential at full hydration, a_f is the apoplastic water fraction, and π_{tlp} is the turgor loss point (Bartlett *et al.*, 2012b). π_o was measured with the osmometer method (π_{osm}) (Bartlett *et al.*, 2012a) in a previous study (Ziegler *et al.*, 2019) and converted to the pressure–volume curve values for π_o and π_{tlp} using the regressions from Bartlett *et al.* (2012a). π_{osm} was measured late in the 2017 dry season (late October–early November), but π_{osm} values measured for the same trees in the 2018 wet season (June) suggest osmotic adjustment minimally impacted our Ψ estimates. Ψ thresholds calculated from

dry season π_{osm} values were only 4% different from thresholds calculated from wet season values, on average, and the thresholds were strongly correlated across species ($r^2 = 0.76\text{--}0.91$, $P < 0.01$, $n = 8$; Fig. S3). We also made the simplifying assumption that $a_f = 0$, as a_f values were not available for these species, which could underestimate the Ψ thresholds (i.e. overestimate resilience). However, a_f is typically low for tropical seasonal forests (mean $a_f = 0.17$; Bartlett *et al.*, 2012b), and comparing $\Psi@PLRC_{35}$ values estimated from $a_f = 0$ and the measured a_f values for the nine species from John *et al.* (2018) and Trueba *et al.* (2019) with available data found these estimates were well-correlated ($r^2 = 0.62$, $P = 0.01$), suggesting that a_f is at most only a moderate driver of variation in these thresholds.

We calculated both low and high thresholds for damage since correlations could differ across thresholds. Lower thresholds for declines in hydraulic conductivity (12%) are typically closer to, and thus more strongly correlated with, leaf water potentials (Bartlett *et al.*, 2016a), while higher thresholds (50%) are generally more strongly correlated with severe drought impacts, such as canopy dieback (Pineda-García *et al.*, 2012). We used 50% as the higher threshold (e.g. $\Psi@PLRC_{50}$) for consistency with the vulnerability curves (see below). The vulnerability curves used 12% as the lower threshold (see below), but Eqn 4 is only applicable to RWC values for which $\Psi \leq \pi_{\text{lp}}$, and 35% was the lowest RWC_d threshold for which all estimated Ψ values were $\leq \pi_{\text{lp}}$. Thus, we used the Ψ values inducing 35% declines in rehydration capacity and chlorophyll fluorescence as our lower thresholds (e.g. $\Psi@PLRC_{35}$). Finally, we used the propagation of error formula to estimate standard deviations for these thresholds from the variances of the osmotic potential measurements and fitted parameters (Methods S1; Table S4).

Hydraulic traits and water potentials

We compiled published values for leaf and stem xylem embolism resistance (Tables 3, S3). Detailed methods are provided in Ziegler *et al.* (2019) and Levionnois *et al.* (2020). Briefly, stem embolism resistance was measured with the flow-centrifugation technique, adapted for long-vesseled species (Burllett *et al.*, 2022). Leaf xylem embolism resistance was measured with the optical light transmission method (Brodribb *et al.*, 2016). The water potential thresholds for 12%, 50%, and 88% declines in stem conductance or nonembolized leaf xylem pixels were extracted from fitted sigmoidal vulnerability curves (i.e. K_{stem} and LXE Ψ_{12} , Ψ_{50} , and Ψ_{88} , respectively). Sample sizes are provided in Table 3.

We also compiled published midday leaf water potential measurements (Ψ_{MD}) from a typical (early October 2018) and a severe dry season (early November 2008) (Stahl *et al.*, 2010; Ziegler *et al.*, 2019). Ψ_{MD} was measured with a pressure chamber (Model 1505D; PMS, Albany, OR, USA) on mature sunlit leaves sampled from the canopy by tree climbers from 11:00 to 14:00 h on sunny days ($n = 3\text{--}6$) (Table 3). Measurements by the nearby Guyaflux tower confirmed vapor pressure deficit was high on these days (> 1.3 kPa) for the dry season at Paracou (Ziegler

et al., 2019). Sampled leaves were immediately bagged and measured within 10 min. Ψ_{MD} was measured for all eight species in 2018 and four species in 2008 (Table 3). Forty years of soil relative extractable water (REW) measurements at Paracou indicate that 2018 was a dry season of typical intensity (i.e. minimum REW = 0.21), while 2008 was the second-driest season on record (i.e. minimum REW = 0.10; Wagner *et al.*, 2011; Aguilos *et al.*, 2019). REW measures the proportion of soil water available for plant uptake; values < 0.4 indicate water stress sufficient to reduce ecosystem productivity at Paracou (Wagner *et al.*, 2011; Stahl *et al.*, 2013).

Stem sap flow

Stem sapflux density was measured continuously on two trees each of four species (*Dicorynia guianensis* Amshoff, *Eperua falcata* Aubl., *Eschweilera sagotiana* Miers, *Pradosia cochlearia* O. Berg) from the end of the rainy season, through the dry season, and 1 month following the return of the rain (i.e. 11 July to 8 December 2018; Table 4). This period includes the typical-intensity 2018 dry season. The same trees were measured for Ψ_{MD} . Each tree was equipped with Granier-type sensors (UP GmbH Headquarters, Ibbenbüren, Germany) consisting of two 20-mm-long and 2-mm-wide probes that were inserted radially into sapwood 10 cm from one another and at an approximate height of 1.5 m. The higher probe was heated and the lower one, acting as the reference, was not. Sapflux density was inferred from the temperature difference between probes (Granier, 1987). The stems, at the location of probe insertion, were covered in a thick multi-layer thermal insulator to minimize any potential bias due to the sun heating the trunk or to water throughfall. Heat flux density was logged every 30 s (CR1000 Datalogger; Campbell Scientific, Shepshed, UK) and averaged every 30 min. Hourly sapflux density was summed to obtain daily sapflux density (D_s ; $\text{kg dm}^{-2} \text{d}^{-1}$). Atmospheric evaporative demand was measured as the cumulative daily potential evapotranspiration (PET; mm d^{-1}), which was calculated from the climate variables measured by the Guyaflux tower with the Penman–Monteith equation.

Stem diameter growth

We used DBH measurements from canopy trees in the Guyaflux tower footprint to characterize growth resilience to drought (Wagner *et al.*, 2012). Fifty-one canopy trees from four of our focal species (*Bocoa prouacensis* Aubl., *D. guianensis*, *E. falcata*, and *E. sagotiana*) were fitted with hand-made metal dendrometer bands and measured for DBH every *c.* 40 d from April 2007 to September 2010, including during the extreme dry season ($n = 4\text{--}25$; Stahl *et al.*, 2010).

Statistical analyses

To evaluate the relationships between resistance to damage during and after drought, we used linear regression to test for correlations between the Ψ thresholds for persistent damage and leaf and stem embolism and midday leaf water potential (Ψ_{MD}) from the typical

Table 3 Drought resistance traits and dry season water potentials compiled from the literature (Ziegler *et al.*, 2019; Levionnois *et al.*, 2020).

Species	LXE Ψ_{50} (MPa)	n_{leaf}	$K_{\text{stem}} \Psi_{50}$ (MPa)	n_{stem}	2008 Ψ_{MD} (MPa)	n_{leaf}	2018 Ψ_{MD} (MPa)	n_{leaf}
<i>Bocoa prouacensis</i>	-4.61	2	-4.29	5	-2.08	3	-1.74	8
<i>Dicorynia guianensis</i>	-3.48	3	-2.38	6	-1.74	4	-1.36	7
<i>Eperua falcata</i>	-3.68	3	-3.86	4	-1.93	5	-1.29	5
<i>Eperua grandiflora</i>	-4.40	3	-6.14	4			-1.29	4
<i>Eschweilera sagotiana</i>	-2.25	3	-2.88	5	-1.74	4	-1.23	7
<i>Lecythis poiteaui</i>	-3.37	2	-2.14	4			-1.82	4
<i>Pradosia cochlearia</i>	-4.51	3	-6.25	5			-2.25	6
<i>Virola michelii</i>	-2.62	3	-5.27	6			-0.88	6

LXE Ψ_{50} are the leaf water potential thresholds for a 50% spread in leaf xylem embolism. $K_{\text{stem}} \Psi_{50}$ are the stem water potential thresholds for a 50% loss of stem hydraulic conductivity. 12% and 88% thresholds are provided in Supporting Information Table S3. Midday leaf water potentials (Ψ_{MD}) were measured in a typical and a historically severe dry season (i.e. 2018 and 2008, respectively; Stahl *et al.*, 2010; Ziegler *et al.*, 2019). n_{leaf} is the number of leaves sampled to measure leaf embolism resistance or water potential and n_{stem} is the number of branches sampled to measure stem hydraulic vulnerability.

Table 4 Leaf water stress, safety margins, and sapflow resilience to drought measured for eight canopy trees from four focal species.

Species	Indiv.	2018 Ψ_{MD} (MPa)	$\Psi_{\text{MD}} - \Psi_{\text{@PLRC}_{35}}$ (MPa)	$\Psi_{\text{MD}} - \Psi_{\text{@PLCF}_{35}}$ (MPa)	Δ_{sapflow} (%)
<i>Dicorynia guianensis</i>	1	-1.13	0.67	0.78	19.9
<i>D. guianensis</i>	2	-1.51	0.29	0.4	-5.3
<i>Eperua falcata</i>	1	-1.15	0.79	1.31	43.1
<i>E. falcata</i>	2	-1.82	0.12	0.64	22.4
<i>Eschweilera sagotiana</i>	1	-1.35	0.53	0.23	-19.6
<i>E. sagotiana</i>	2	-1.43	0.45	0.15	-14.8
<i>Pradosia cochlearia</i>	1	-2.85	-0.5	0.07	-2.0
<i>P. cochlearia</i>	2	-1.28	1.07	1.64	21.6

Ψ_{MD} is the midday leaf water potential from the typical (2018) dry season. Safety margins are calculated as the difference between Ψ_{MD} and the thresholds for persistent damage to rehydration capacity and photochemical function and resistance to leaf and stem embolism (e.g. $\Psi_{\text{MD}} - \Psi_{\text{@PLRC}_{35}}$). Ψ_{MD} is measured for the individual trees, and the drought resilience and resistance thresholds are the values for each species (Table 2). Δ_{sapflow} is the percent change in cumulative daily sapflow, calculated at the mean daily potential evapotranspiration (i.e. 7.5 mm d⁻¹), before and after the 2018 dry season (i.e. (postdrought - predrought)/predrought). Negative Δ_{sapflow} values indicate that whole-plant sap flow remained lower in the wet period after the 2018 dry season, compared with the preceding wet period. Safety margins for incipient (12%) embolism are provided in Supporting Information Table S5.

(2018) and severe (2008) dry seasons. For all linear regressions, we conducted standard tests for normality and heteroscedasticity to ensure these analyses were appropriate.

To characterize species' risk of damage during and after drought, we used mean Ψ_{MD} values to calculate safety margins from species' thresholds for leaf and stem embolism and persistent damage to rehydration capacity and photochemical function (e.g. $\Psi_{\text{MD}} - \Psi_{\text{@PLRC}_{35}}$). We used *t*-tests to evaluate whether the safety margins for persistent damage were significantly different from 0 in either year.

We then tested whether larger safety margins predict greater resilience in sap flow. We used REW to define periods with high soil moisture (i.e. REW \geq 0.8) before and after the 2018 dry season (i.e. a 'wet' and a 'recovery' period, respectively). Then, we fitted linear regressions between cumulative daily potential evapotranspiration (PET) and daily sapflux density (D_s) for each individual to evaluate plant capacity to increase transpiration to meet evaporative demand. We fitted separate regressions for the wet and recovery periods for each individual and used the regressions to calculate daily sapflux density in each period at the mean daily PET over both periods (7.5 mm d⁻¹), and recovery as the percent change in daily sapflux density

at mean PET (Δ_{sapflow}) in the recovery compared with the wet period. Individual safety margins were calculated from individual Ψ_{MD} measurements and species thresholds for embolism and persistent damage.

Finally, we tested whether larger safety margins predict greater resilience in diameter growth after drought. We calculated safety margins from species thresholds for embolism and persistent damage and species mean Ψ_{MD} values in the severe 2008 dry season, the driest point of the dendrometer monitoring period. We used a hierarchical Bayesian model to predict the growth rate for each individual *i* of species *s* for the wet season of year *t* ($G_{i,s,t}^{\text{wet}}$) as a function of the safety margins (Trait_{*s*}) and drought intensity of the previous dry season (D_{t-1})

$$G_{i,s,t}^{\text{wet}} \sim N((\alpha_{i,s} + \beta_s D_{t-1}), \sigma^2) \quad \text{Eqn 5a}$$

$$\beta_s \sim N((\beta + \gamma \text{Trait}_s), \sigma_D^2) \quad \text{Eqn 5b}$$

D_{t-1} represents cumulative stress over the dry season and was calculated as $\sum_0^d (\text{REW}_d - 0.4)$, the cumulative difference between the daily REW (REW_{*d*}) and threshold for drought

stress at Paracou (REW = 0.4). $\alpha_{i,s}$, β , and γ are fitted parameters. $\alpha_{i,s}$ is the wet season growth rate of individual i of species s after an average dry season. β is the average effect of dry season intensity on wet season growth across species, and γ is the effect of the safety margin on the wet season growth response to dry season intensity. β_s represents the effect of dry season intensity on growth in the following wet season for each species s . A more negative β_s indicates a species' growth rate is more strongly reduced after an intense dry season, and thus, less resilient to drought. We tested whether larger safety margins were associated with a less negative β_s . The model was fitted with an adaptive form of the Hamiltonian Monte Carlo sampling (Carpenter *et al.*, 2017) using the RSTAN package (Stan Development Team, 2018) and weakly informative priors (Methods S1).

Results

Thresholds for persistent declines in leaf rehydration capacity and photochemical function

Across the eight tropical species, 35% and 50% declines in leaf rehydration capacity (PLRC₃₅ and PLRC₅₀) occurred at Ψ thresholds of -2.02 ± 0.08 MPa and -2.61 ± 0.09 MPa, respectively (mean \pm standard error) (Table 2; Fig. 3a). 35% and 50% declines in chlorophyll fluorescence (PLCF₃₅ and PLCF₅₀) occurred at Ψ thresholds of -2.43 ± 0.20 MPa and -3.14 ± 0.36 MPa (Table 2; Fig. 3a). The thresholds for 35% fluorescence loss were significantly more negative than for rehydration capacity (paired t -tests, $P = 0.04$, $n = 8$), while $\Psi@PLRC_{50}$ and $\Psi@PLCF_{50}$ were not significantly different ($P = 0.13$, $n = 8$). The PLRC and PLCF thresholds were not correlated ($r^2 = 0.01$, $P > 0.05$, $n = 8$; Fig. 3b).

Resilience to persistent leaf photochemical damage is correlated with leaf embolism resistance and water stress in the dry season

The species with greater resilience to persistent photochemical damage were more resistant to leaf xylem embolism and exhibited more negative water potentials in the dry season. $\Psi@PLCF_{35}$ and $\Psi@PLCF_{50}$ were correlated with thresholds for severe leaf xylem embolism (LXE Ψ_{50} and Ψ_{88} ; $r^2 = 0.50$ – 0.56 , $P < 0.05$, $n = 8$), but not incipient embolism (LXE Ψ_{12} ; $r^2 = 0$ – 0.19 , $P \geq 0.2$; Table 5; Fig. 4a). Conversely, neither $\Psi@PLRC_{35}$ nor $\Psi@PLRC_{50}$ was correlated with vein embolism resistance, though the correlations with LXE Ψ_{50} were marginally significant (both $P = 0.07$, $n = 8$; Table 5; Fig. 4b). None of the $\Psi@PLRC$ or $\Psi@PLCF$ thresholds were correlated with stem embolism resistance ($P > 0.2$; Table 5).

$\Psi@PLCF_{35}$ was correlated with midday leaf water potentials (Ψ_{MD}) in both the typical (2018) and severe (2008) dry seasons ($r^2 = 0.45$ and 0.94 , $P < 0.05$, $n = 8$ and 4 , respectively; Table 5; Fig. 4c). $\Psi@PLCF_{50}$ was correlated with Ψ_{MD} in the extreme ($r^2 = 0.88$, $P = 0.04$, $n = 4$) but not the typical dry season ($P = 0.2$, $n = 8$), while the opposite was true for $\Psi@PLRC_{50}$ ($r^2 = 0.61$, $P = 0.02$ for 2018, $P = 0.1$ for 2008; Table 5; Fig. 4d). $\Psi@PLRC_{35}$ was not correlated with Ψ_{MD} in either 2008 or 2018 ($P > 0.05$; Table 5).

Safety margins for persistent damage are positive in a typical dry season

The safety margins for $\Psi@PLRC_{35}$ and $\Psi@PLCF_{35}$ were significantly > 0 in the typical dry season (i.e. 0.46 ± 0.13 MPa for $\Psi@PLRC_{35}$ and 0.85 ± 0.24 MPa for $\Psi@PLCF_{35}$, $P < 0.01$, $n = 8$; Fig. 5). For the four species that were measured in both

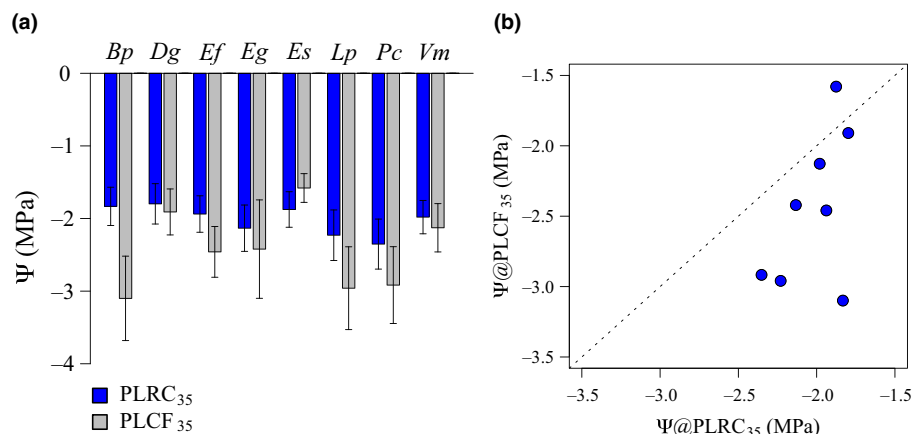


Fig. 3 Water potential (Ψ) thresholds at which the eight tropical species lose 35% of their leaf rehydration capacity (PLRC₃₅, blue bars) or maximum quantum efficiency of photosystem II (PLCF₃₅, gray bars) in rehydrated compared with saturated leaves (a) and the relationship between PLRC₃₅ and PLCF₃₅ (b) (Table 2). Abbreviations are the first letter of each genus and species (*Bocoa prouacensis*, *Dicorynia guianensis*, *Eperua falcata*, *E. grandiflora*, *Eschweilera sagotiana*, *Lecythis poiteaui*, *Pradosia cochlearia*, and *Virola michelii*). Error bars are SDs (see Supporting Information Methods S1). Dotted line is the 1 : 1 line. We hypothesized that the drought resilience traits would be correlated if losing rehydration capacity prevents leaves from regaining photochemical function (Fig. 2, #2), or leaves have been selected to stop repairing damage in multiple functions at similar water stress thresholds (Fig. 2, #5). However, contrary to expectation, PLRC₃₅ and PLCF₃₅ were not significantly correlated ($r^2 = 0.01$, $P = 0.19$, $n = 8$).

Table 5 r^2 values for the correlations between the drought resilience traits (i.e. water potential thresholds for persistent damage to rehydration capacity and photochemical function), drought resistance traits (i.e. water potential thresholds for leaf xylem embolism and declines in stem hydraulic conductance during dehydration), and water stress (i.e. midday leaf water potentials during a typical (2018) and severe (2008) dry season) *in situ* in a natural tropical ecosystem.

	$\Psi@PLRC_{35}$ (MPa)	$\Psi@PLRC_{50}$ (MPa)	$\Psi@PLCF_{35}$ (MPa)	$\Psi@PLCF_{50}$ (MPa)
LXE Ψ_{12} (MPa)	0	0.01	0	0.19
LXE Ψ_{50} (MPa)	0	0.35	0.50*	0.56*
LXE Ψ_{88} (MPa)	0	0.31	0.52*	0.54*
$K_{stem} \Psi_{12}$ (MPa)	0.02	0.01	0	0.02
$K_{stem} \Psi_{50}$ (MPa)	0.07	0	0	0.05
$K_{stem} \Psi_{88}$ (MPa)	0.10	0	0	0.06
2018 Ψ_{MD} (MPa)	0.25	0.61*	0.45*	0.09
2008 Ψ_{MD} (MPa)	0	0.51	0.94*	0.88*

Asterisks and bold indicate significant correlations ($P < 0.05$). $n = 8$, except for the correlations with the 2008 midday water potentials, where $n = 4$ (Table 3).

years, Ψ_{MD} decreased from -1.40 ± 0.11 MPa to -1.87 ± 0.08 MPa in 2018 and 2008, respectively. In the extreme dry season, safety margins decreased and became close to zero for $\Psi@PLRC_{35}$ and $\Psi@PLCF_{35}$ (-0.01 ± 0.08 MPa and 0.39 ± 0.25 MPa, respectively) and were not statistically different from 0 ($P > 0.05$; Fig. 5).

Drought resilience in sap flow is correlated with safety margins for persistent photochemical damage and leaf xylem embolism

The Amazonian trees with smaller safety margins for photochemical damage and leaf xylem embolism resistance exhibited greater reductions in sap flow between the wet and recovery periods (i.e. the 2–3-wk periods with high soil moisture before and after the 2018 dry season, respectively). Sap flow and safety margins were measured for eight individuals of four species (Tables 4, S5). Sap flow at the mean PET (i.e. 7.5 mm d^{-1}) was lower in the recovery than in the wet period for half of the individuals (Table 4; Fig. 6). $\Delta_{sapflow}$, the percent change in sap flow at mean PET between the wet and recovery periods, was significantly correlated with the safety margins for persistent damage to F_v/F_m ($r^2 = 0.76$ – 0.79 for $\Psi@PLCF_{35}$ and $\Psi@PLCF_{50}$, $P < 0.01$, $n = 8$) and leaf xylem embolism resistance ($r^2 = 0.55$ – 0.82 for LXE Ψ_{12} , Ψ_{50} and Ψ_{88} , $P < 0.05$, $n = 8$; Table 6; Fig. 7). $\Delta_{sapflow}$ was not correlated with Ψ_{MD} or the safety margins for $\Psi@PLRC$ or stem embolism resistance (Table 6).

Safety margins for photochemical damage and embolism were associated, but not significantly correlated, with drought resilience in stem growth

We observed a general trend that stem diameter growth rates in the 2007–2010 wet seasons were inversely related to the intensity of the preceding dry season and that growth reductions were larger in the species with smaller safety margins, though these

relationships were not significant for our small species set ($n = 4$; Tables S6, S7; Fig. S3). We defined species' growth resilience from the fitted slopes for relationships between dry season intensity and growth in the subsequent wet season (β_s). β_s values were typically negative, indicating wet season growth rates were reduced proportionally to the intensity of the preceding dry season, and more negative, indicating larger reductions in growth, in the species with smaller safety margins for leaf and stem embolism and persistent photochemical damage, although the relationship with the safety margin for rehydration capacity was in the opposite direction than expected (Tables S6, S7; Fig. S3). However, the 95% credibility intervals for β_s overlapped with 0, indicating species' growth responses were not significantly different from 0.

Discussion

This study is the first to show that the thresholds for persistent damage to photochemical function are an integral part of broader plant drought tolerance. Drought resilience in leaf photochemistry was strongly coordinated with drought resistance across co-occurring species within a tropical forest. The species with more negative thresholds for persistent photochemical damage were more resistant to leaf vein embolism and exhibited more negative water potentials in the dry season (Table 5; Fig. 4a,c). Leaf resilience to photochemical damage also emerged as a promising functional trait to characterize whole-plant drought resilience. The plants that maintained larger safety margins for persistent photochemical damage exhibited greater resilience in sap flow (Table 6; Fig. 7). The coordination between leaf and plant drought resilience and strong reductions in the safety margins for photochemical damage in the severe dry season (Fig. 5) suggest that the increased drought severity projected for the American tropics will hinder plant and ecosystem carbon uptake beyond drought events. The coordination between resistance and resilience suggests that species' differences in performance during drought will be perpetuated after drought, potentially accelerating shifts in forest composition.

Potential mechanisms driving relationships between leaf drought resistance and resilience

The positive correlations between $\Psi@PLCF_{35}$ and leaf vein embolism resistance could reflect a direct effect of embolism on F_v/F_m (Fig. 2, #1, 2) or an evolutionary coordination between leaf xylem and photochemical drought responses (Figs 2, #4, 4a). In intact plants that have been dehydrated and rewatered, embolized veins typically fail to refill, which may prevent the downstream mesophyll tissue from fully rehydrating (Johnson *et al.*, 2018; Brodrigg *et al.*, 2021). Thus, embolism could have prevented recovery in F_v/F_m in this study, driving a causative relationship between $\Psi@PLCF_{35}$ and LXE Ψ_{50} . However, rehydrated excised leaves can at least partly refill embolized veins through capillarity (Johnson *et al.*, 2018). Instead, dehydration could directly impact F_v/F_m by physically deforming the chloroplasts and increasing oxidative damage to the electron transport

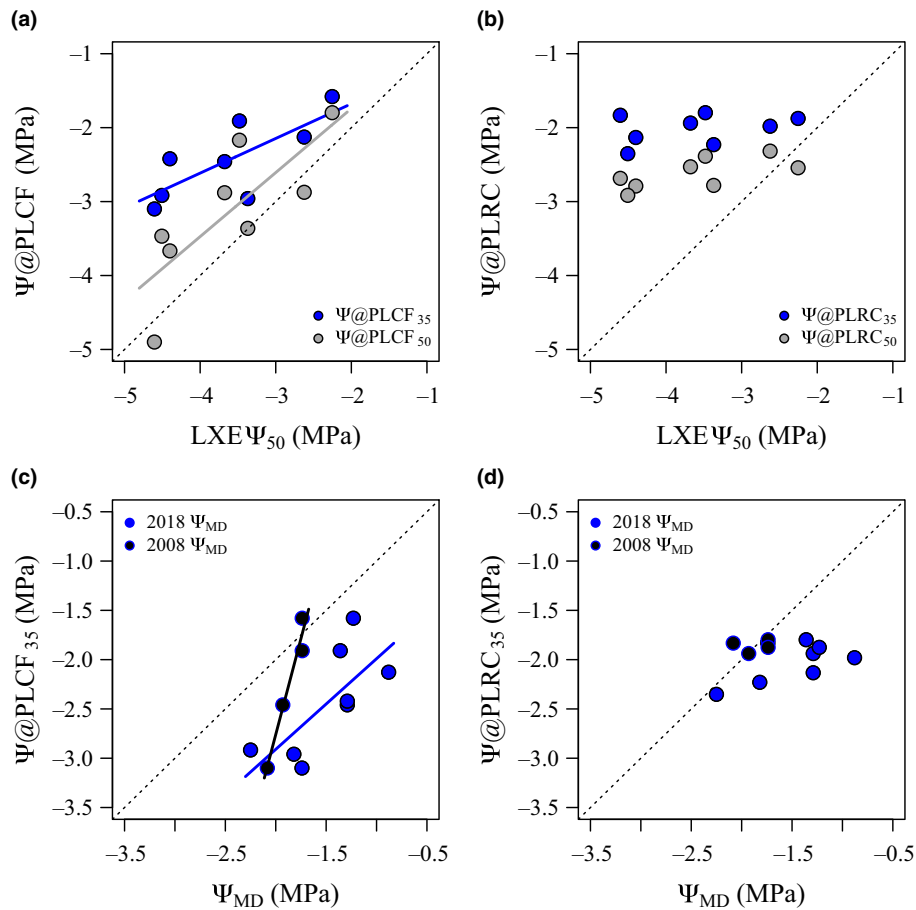


Fig. 4 Relationships between the leaf drought resilience traits, leaf vein embolism resistance (a, b), and dry season water potentials (c, d) across the eight rainforest species. The water potential thresholds for persistent declines in F_v/F_m are shown in the left panels ($\Psi@PLCF$, a, c) and thresholds for persistent declines in rehydration capacity are shown on the right ($\Psi@PLRC$, b, d). The blue and gray points show thresholds for 35% and 50% declines, respectively. $LXE \Psi_{50}$ is the leaf water potential threshold for 50% embolism spread in the leaf veins (a, b). Ψ_{MD} is the midday leaf water potential in the 2018 or 2008 dry season (c, d). Solid lines are statistically significant correlations. We hypothesized that leaf embolism resistance and the drought resilience traits would be causatively related if embolism prevents leaves from rehydrating and, thus, regaining F_v/F_m , or simply correlated (Fig. 2, #1, 2), if leaves have evolved to stop repairing damage as the veins embolize (Fig. 2, #3, 4) (Brodrribb *et al.*, 2021; Trifilò *et al.*, 2021). We also hypothesized the drought resilience traits and Ψ_{MD} would be correlated if leaves regulate water potential to avoid persistent damage (Fig. 2, #6, 7). We found that the higher thresholds (50% and 88%) for leaf embolism resistance were significantly correlated with both thresholds for persistent damage to F_v/F_m ($\Psi@PLCF$, $r^2 = 0.50$, $P < 0.01$, a) but not rehydration capacity ($\Psi@PLRC$, $r^2 = 0.01$, $P = 0.4$, b) (Table 5). Greater photochemical resilience was significantly correlated with more negative water potentials in both dry seasons (i.e. for $\Psi@PLCF_{35}$, $r^2 = 0.45$ and 0.94 , $P < 0.05$, $n = 8$ and 4 for 2018 and 2008, c) (Table 5).

chain (Moran *et al.*, 1994; Zhang *et al.*, 2015), or indirectly reduce F_v/F_m by triggering chloroplast degradation as a part of leaf senescence (Munné-Bosch *et al.*, 2001; Vollenweider *et al.*, 2016). Thus, the correlations in this study could reflect independent selection for xylem and photochemical drought resistance. Plants could be selected to stop protecting or repairing the photochemical machinery or to initiate leaf senescence at the water stress thresholds for vein embolism, to reduce resource allocation to dysfunctional leaves. In this case, refilling through capillarity would not reverse the chloroplast damage or active degradation due to dehydration that coincides with embolism. Future work is needed to determine whether photochemical resistance to persistent damage is directly influenced by vein embolism, or indirectly set by other mechanisms coordinated with hydraulics, including reactive oxygen species production and scavenging and aspects of thylakoid membrane composition and

structure (Fan *et al.*, 2009; Saglam *et al.*, 2011; X.-K. Guan *et al.*, 2015; Iqbal *et al.*, 2019).

Greater resilience to persistent photochemical damage and resistance to leaf xylem embolism were also coordinated with reaching more negative leaf water potentials in the dry season (Ψ_{MD} ; Table 5; Fig. 4c). These relationships are consistent with the expectation that plants regulate water potential to avoid persistent damage (Fig. 2, #7) and indicate that plants adapt to greater dehydration by increasing resistance to damage both during and after drought. The resistant/resilient species could reach more negative water potentials because these traits are coordinated with drought-resistant stomatal behavior, where stomata remain open under more negative water potentials, or because these species are associated with drier microhabitats within forests (e.g. shallower rooting depths and drier topographic associations; Bartlett *et al.*, 2016b). These traits were correlated with stomatal

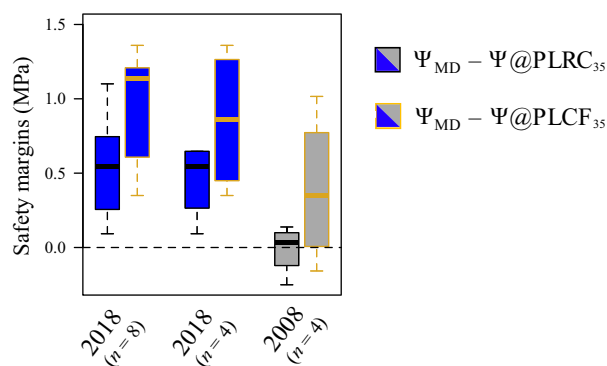


Fig. 5 Safety margins for rehydration capacity and photochemical function in a typical (2018, blue bars) and an extreme (2008, gray bars) dry season. Black outlines indicate safety margins for rehydration capacity ($\Psi_{MD} - \Psi@PLRC_{35}$) and gold outlines indicate margins for photochemical damage ($\Psi_{MD} - \Psi@PLCF_{35}$). Left blue bars show mean safety margins for all eight species measured in 2018, and the middle blue bars show the four species measured in both seasons. Safety margins were significantly > 0 in the typical dry season, but not the extreme dry season.

behavior across species from biomes world-wide (Trueba *et al.*, 2019), but variation in stomatal behavior or rooting depth across co-occurring species at Paracou is largely unknown.

Even though rehydration capacity was more vulnerable to persistent damage than photochemistry, and thus theoretically more limiting to leaf function, rehydration capacity was not correlated with $\Psi@PLCF$, vein embolism resistance, or Ψ_{MD} , contrary to expectation (Fig. 2, #1–3, 5). This could reflect the limited variation in $\Psi@PLRC$ in these species (i.e. $\Psi@PLRC_{35}$ ranges from -1.8 to -2.4 MPa, while $\Psi@PLCF_{35}$ ranges from -1.6 to -3.1 MPa; Fig. 3a). Disruptions to the electron transport chain reactions occur under more severe dehydration than cell wall collapse and deformation (Lamont & Lamont, 2000), so F_v/F_m could remain high even when rehydration capacity is reduced as long as rehydrated RWC is above the thresholds for photochemical damage, decoupling $\Psi@PLCF$ from $\Psi@PLRC$ (Fig. 3b). The weak relationships between $\Psi@PLRC$ and $\Psi@PLCF$ are also consistent with the hypothesis that water storage and photosynthesis are specialized to different tissues, since most of leaf chlorophyll fluorescence originates in the palisade mesophyll (Gould *et al.*, 2002), while most of the water released during dehydration is from the spongy mesophyll (Binks *et al.*, 2016; Xiong & Nadal, 2020). This hypothesis is also supported by findings from other species. For *Quercus robur*, severe drought caused widespread cell collapse and wall buckling in the spongy and palisade mesophyll, and F_v/F_m remained low for several weeks after rehydration (Arend *et al.*, 2013; Vollenweider *et al.*, 2016). Conversely, for *Quercus petraea* and *Quercus pubescens* at the same site, cellular damage was concentrated in the spongy mesophyll while the palisade remained largely intact, and F_v/F_m recovered to saturated values within days of rehydration. Further, the absence of correlations between rehydration capacity, embolism resistance, and water potential could indicate that losing rehydration capacity is a weaker constraint on leaf function than photochemical function, and thus, there has been less selective pressure coordinating these traits (Table 5; Fig. 4b,d). For example, some

angiosperms exhibit a close hydraulic connection between the veins and epidermis that allows some water transport to bypass the mesophyll and prioritize rehydrating the epidermis, which could allow the stomata to recover turgor and reopen before the spongy mesophyll has fully rehydrated (Zwieniecki *et al.*, 2007).

Potential mechanisms linking leaf to whole-plant drought resilience

Leaf safety margins for persistent photochemical damage and vein embolism were positively correlated with drought resilience in plant sap flow (Table 6; Fig. 7), consistent with the expectation that plants with larger safety margins avoid persistent damage to leaf function and, potentially, triggering significant leaf senescence, allowing canopy-scale gas exchange to return to pre-drought levels more quickly at the beginning of the postdrought wet season (Fig. 2, #9). In half of the individuals, sap flow was higher after drought than before, suggesting that avoiding leaf damage facilitated new growth and quickly increased canopy size and, thus, transpiration and sap flow, relative to the predrought period (Blackman *et al.*, 2009; Table 4). The leaf area index at Paracou typically peaks early in the wet season, indicating this is a period of rapid growth for many trees at this site (Wagner *et al.*, 2013). An important effect of leaf senescence on sapflow resilience would suggest that resilience varies with phenology. Cumulative leaf damage over multiple droughts reduced resilience in carbon gain for conifers with long leaf lifespans, while the opposite extreme, drought-deciduousness, could also reduce sapflow resilience, since the entire canopy area must be replaced after drought (Forner *et al.*, 2014; Song *et al.*, 2022). However, the timing and intensity of leaf senescence can be highly variable across individuals, even within drought-deciduous species, indicating more work is needed to relate individual leaf litterfall dynamics to sapflow resilience (Maréchaux *et al.*, 2018). Moreover, resilience could also be affected by rooting depth. Rainfall would likely rehydrate trees with shallower roots more quickly, but our findings suggest that deeper rooting could promote resilience by maintaining larger safety margins for photochemical damage during drought. Finally, contrary to expectation, the safety margins for $\Psi@PLCF_{35}$ and incipient embolism (LXE Ψ_{12}) were positive even in the individuals where sap flow declined (Table S5). The safety margins for LXE Ψ_{12} were large even in the trees with reduced sap flow (0.55–1.19 MPa), but narrower for $\Psi@PLCF_{35}$ (0.07–0.40 MPa), even though 35% is a higher threshold, suggesting that embolism was negligible, but water potentials could have crossed lower thresholds for photochemical damage (e.g. $\Psi@PLCF_{10}$; Table S5; Fig. 7). Future work relating leaf damage to litterfall and leaf and plant gas exchange is needed to determine the mechanisms relating safety margins to sapflow drought resilience.

Stem diameter growth in the wet season was generally more resilient to intense drought in the preceding dry season in the species with larger safety margins for embolism and persistent photochemical damage, though this trend was not significant in this small species set (Table S6; Fig. S3). Persistent leaf damage could reduce stem growth after drought by limiting carbon

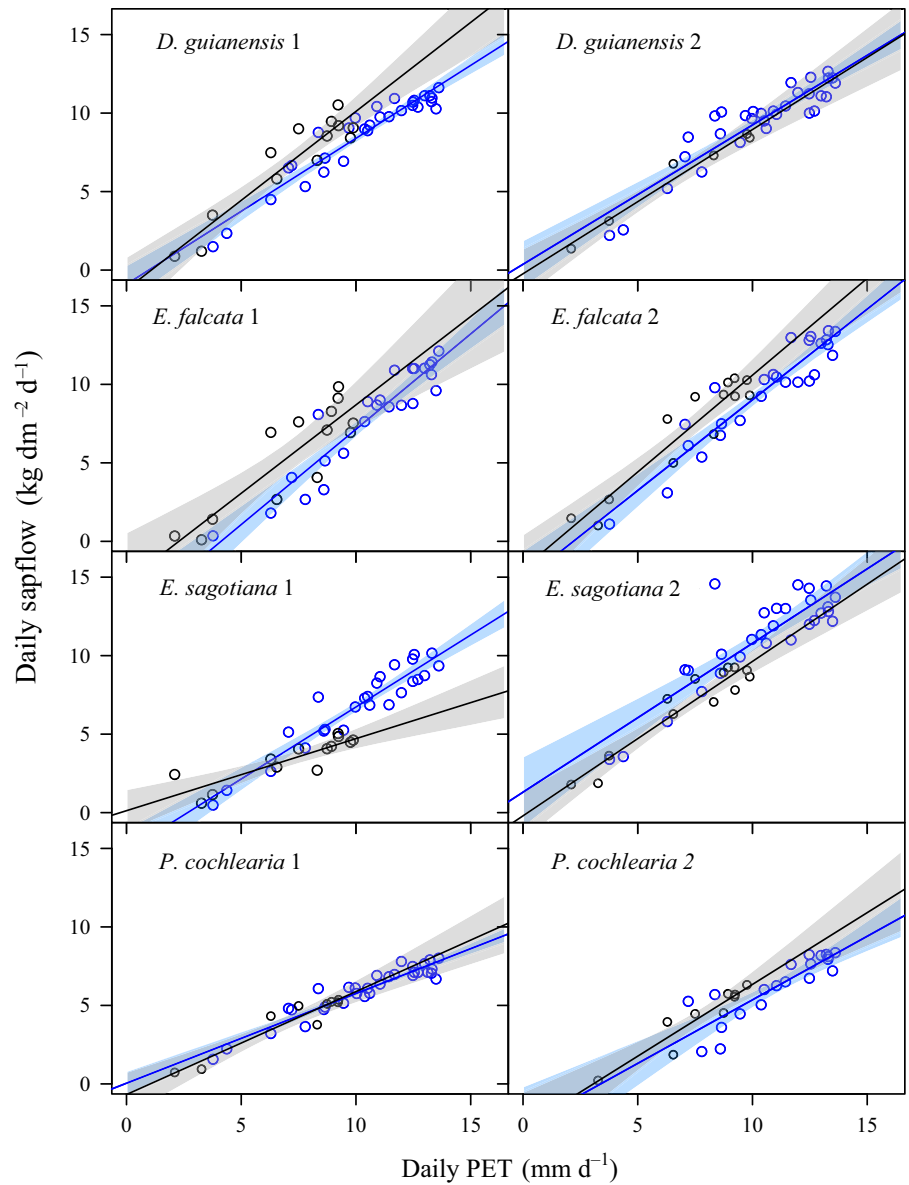


Fig. 6 Comparing relationships between evaporative demand (cumulative daily potential evapotranspiration; PET) and transpiration (cumulative daily sap flow) under well-watered conditions before (blue circles) and after (black circles) the 2018 regular dry season. Each panel is one individual tree. Solid lines show best-fit correlations. Colored areas show 95% confidence intervals around each correlation.

assimilation or increasing the allocation of assimilated carbon or stored carbohydrates to repairing damaged tissues or replacing abscised leaves (Trugman *et al.*, 2018; Kannenberg *et al.*, 2019; Fig. 2, #12, 13). Our findings suggest that measuring leaf drought resilience could inform predictions for stem diameter growth after drought, and thus, it is a valuable direction for future work to robustly test these relationships across a large species set in more ecosystems.

Implications for tropical forest responses to climate change

Climate change is predicted to exacerbate drought in the Eastern Amazon by reducing mean annual precipitation and increasing precipitation seasonality (i.e. intensifying the wet and dry seasons; Duffy *et al.*, 2015). Our findings suggest several mechanisms by which persistent leaf damage could reduce future carbon sequestration in these forests. First, persistent photochemical

damage or increased leaf senescence could reduce photosynthesis, not only in the dry season but also at the beginning of the wet season, when carbon assimilation should be high (K. Guan *et al.*, 2015). Second, accelerating leaf senescence could reduce long-term carbon sequestration by increasing carbon allocation to the rapid-cycling leaf biomass pool relative to woody biomass (Galbraith *et al.*, 2013; Yang *et al.*, 2021). Finally, failing to recover a positive carbon balance could increase tree mortality in the years after severe droughts (Trugman *et al.*, 2018). The positive coordination between drought resistance and resilience also suggests that species' differences in performance during drought will be perpetuated afterward, accelerating the expected shifts in forest composition toward drought-resistant/resilient species (Fig. 4b,d; Bartlett *et al.*, 2019). Our findings also point to remote sensing for solar-induced chlorophyll fluorescence as a promising approach to monitor immediate and persistent drought impacts on tropical forest productivity (Lee *et al.*, 2013).

Table 6 r^2 values for the correlations between the percent recovery in sap flow after, compared with before, the 2018 dry season (Δ_{sapflow}), dry season midday leaf water potentials (Ψ_{MD}), and the safety margins between Ψ_{MD} and the thresholds for persistent damage and hydraulic damage during dehydration (e.g. $\Psi_{\text{MD}} - \Psi@PLRC_{35}$).

	r^2
Ψ_{MD}	0
$\Psi_{\text{MD}} - \Psi@PLRC_{35}$	0.10
$\Psi_{\text{MD}} - \Psi@PLRC_{50}$	0.04
$\Psi_{\text{MD}} - \Psi@PLCF_{35}$	0.76**
$\Psi_{\text{MD}} - \Psi@PLCF_{50}$	0.79**
$\Psi_{\text{MD}} - \text{LXE } \Psi_{12}$	0.82**
$\Psi_{\text{MD}} - \text{LXE } \Psi_{50}$	0.67**
$\Psi_{\text{MD}} - \text{LXE } \Psi_{88}$	0.55*
$\Psi_{\text{MD}} - K_{\text{stem}} \Psi_{12}$	0.02
$\Psi_{\text{MD}} - K_{\text{stem}} \Psi_{50}$	0.14
$\Psi_{\text{MD}} - K_{\text{stem}} \Psi_{88}$	0.10

Asterisks and bold text indicate significant correlations (*, $P < 0.05$; **, $P < 0.01$). $n = 8$ canopy trees (Table 4).

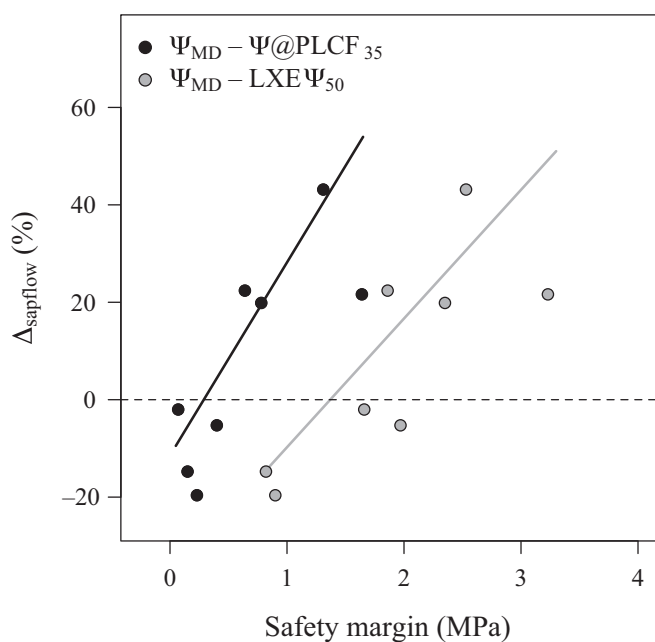


Fig. 7 Correlations between recovery in sap flow and the safety margins for persistent photochemical damage ($\Psi_{\text{MD}} - \Psi@PLCF_{35}$, black circles) and leaf vein embolism ($\Psi_{\text{MD}} - \text{LXE } \Psi_{50}$, gray circles) in eight individuals of our four focal species (Table 4). $\text{LXE } \Psi_{50}$ is the leaf water potential threshold for 50% embolism spread in the leaf veins. Δ_{sapflow} is the percent change in cumulative daily sap flow, calculated at the mean daily PET, before and after the 2018 dry season (i.e. postdrought – predrought)/predrought). Ψ_{MD} is the midday water potential from the 2018 dry season. Δ_{sapflow} and Ψ_{MD} are measured for each individual, and $\text{LXE } \Psi_{50}$ and $\Psi@PLCF_{35}$ are species means. Negative Δ_{sapflow} values indicate that sap flow is lower in the recovery than the in wet period. We hypothesized that plants with larger safety margins would avoid persistent reductions in leaf-level gas exchange, and potentially triggering leaf senescence, allowing canopy-scale gas exchange to quickly return to predrought levels after drought (Fig. 2, #10, 11). Consistent with this hypothesis, Δ_{sapflow} was significantly positively correlated with the safety margins for all thresholds for $\Psi@PLCF$ ($r^2 = 0.76\text{--}0.79$, $P < 0.01$, $n = 8$) and LXE ($r^2 = 0.55\text{--}0.82$, $P < 0.05$, $n = 8$). However, contrary to expectation, Δ_{sapflow} was not correlated with either threshold for $\Psi@PLRC$ ($r^2 = 0.04\text{--}0.1$, $P > 0.05$, $n = 8$).

Acknowledgements

This work has benefited from support of a grant from Investissement d'Avenir grants of the ANR (CEBA:ANR-10-LABX-25-01). MKB was also supported by the UC Davis Viticulture and Enology Department and College of Agriculture and Natural Resources. We thank Valentine Alt, Jocelyn Cazal, and Ariane Mirabel for their assistance with tree climbing and sampling. We would like to thank Benoit Burban for the setting up of the sapflow sensors and his technical assistance. Part of this work was carried out at the Jet Propulsion Laboratory, California Institute of Technology, under a contract with the National Aeronautics and Space Administration (NASA).

Competing interests

None declared.

Author contributions

MKB conceived of the study. MKB, CF, C Stahl, SC, SJ and JC developed the study design. MKB and CF led manuscript preparation. LS, ST, GJ, C Scoffoni and PH contributed to methods development for the trait measurements. MKB, CF, C Stahl, SC, CZ and SL conducted the trait measurements. CZ, IM and DB monitored and analyzed sapflow recovery. GD, BH and FHW monitored and analyzed secondary growth. GD conducted growth modeling. All authors contributed to designing the analyses and revising the manuscript.

ORCID

Megan K. Bartlett <https://orcid.org/0000-0003-0975-8777>
 Damien Bonal <https://orcid.org/0000-0001-9602-8603>
 Jérôme Chave <https://orcid.org/0000-0002-7766-1347>
 Sabrina Coste <https://orcid.org/0000-0003-3948-4375>
 Géraldine Derroire <https://orcid.org/0000-0001-7239-2881>
 Claire Fortunel <https://orcid.org/0000-0002-8367-1605>
 Bruno Héroult <https://orcid.org/0000-0002-6950-7286>
 Patrick Heuret <https://orcid.org/0000-0002-7956-0451>
 Steven Jansen <https://orcid.org/0000-0002-4476-5334>
 Grace John <https://orcid.org/0000-0002-8045-5982>
 Sébastien Levionnois <https://orcid.org/0000-0002-7217-9762>
 Isabelle Maréchaux <https://orcid.org/0000-0002-5401-0197>
 Lawren Sack <https://orcid.org/0000-0002-7009-7202>
 Christine Scoffoni <https://orcid.org/0000-0002-2680-3608>
 Clément Stahl <https://orcid.org/0000-0001-5411-1169>
 Santiago Trueba <https://orcid.org/0000-0001-8218-957X>
 Fabien H. Wagner <https://orcid.org/0000-0002-9623-1182>
 Camille Ziegler <https://orcid.org/0000-0002-0855-1347>

Data availability

The data supporting the findings of this study are available as [Supporting Information](#).

REFERENCES

- Abid M, Tian Z, Ata-Ul-Karim ST, Wang F, Liu Y, Zahoor R, Jiang D, Dai T. 2016. Adaptation to and recovery from drought stress at vegetative stages in wheat (*Triticum aestivum*) cultivars. *Functional Plant Biology* 43: 1159–1169.
- Aguilos M, Stahl C, Burban B, Hérault B, Courtois E, Coste S, Wagner F, Ziegler C, Takagi K, Bonal D. 2019. Interannual and seasonal variations in ecosystem transpiration and water use efficiency in a tropical rainforest. *Forests* 10: 14.
- Anderegg WRL, Anderegg LDL, Berry JA, Field CB. 2014. Loss of whole-tree hydraulic conductance during severe drought and multi-year forest die-off. *Oecologia* 175: 11–23.
- Anderegg WRL, Schwalm C, Biondi F, Camarero JJ, Koch G, Litvak M, Ogle K, Shaw JD, Shevliakova E, Williams AP *et al.* 2015. Pervasive drought legacies in forest ecosystems and their implications for carbon cycle models. *Science* 349: 528–532.
- Arend M, Brem A, Kuster TM, Günthardt-Goerg MS. 2013. Seasonal photosynthetic responses of European oaks to drought and elevated daytime temperature: photosynthetic responses to drought and elevated temperature. *Plant Biology* 15: 169–176.
- Bartlett MK, Detto M, Pacala SW. 2019. Predicting shifts in the functional composition of tropical forests under increased drought and CO₂ from trade-offs among plant hydraulic traits. *Ecology Letters* 22: 67–77.
- Bartlett MK, Scoffoni C, Ardy R, Zhang Y, Sun S, Cao K, Sack L. 2012a. Rapid determination of comparative drought tolerance traits: using an osmometer to predict turgor loss point. *Methods in Ecology and Evolution* 3: 880–888.
- Bartlett MK, Scoffoni C, Sack L. 2012b. The determinants of leaf turgor loss point and prediction of drought tolerance of species and biomes: a global meta-analysis. *Ecology Letters* 15: 393–405.
- Bartlett MK, Klein T, Jansen S, Choat B, Sack L. 2016a. The correlations and sequence of plant stomatal, hydraulic, and wilting responses to drought. *Proceedings of the National Academy of Sciences, USA* 113: 13098–13103.
- Bartlett MK, Zhang Y, Yang J, Kreidler N, Sun S-W, Lin L, Hu Y-H, Cao K-F, Sack L. 2016b. Drought tolerance as a driver of tropical forest assembly: resolving spatial signatures for multiple processes. *Ecology* 97: 503–514.
- Binks O, Meir P, Rowland L, Costa ACL, Vasconcelos SS, Oliveira AAR, Ferreira L, Christoffersen B, Nardini A, Mencuccini M. 2016. Plasticity in leaf-level water relations of tropical rainforest trees in response to experimental drought. *New Phytologist* 211: 477–488.
- Blackman CJ, Brodrribb TJ, Jordan GJ. 2009. Leaf hydraulics and drought stress: response, recovery and survivorship in four woody temperate plant species. *Plant, Cell & Environment* 32: 1584–1595.
- Brodrribb T, Brodersen CR, Carriqui M, Tonet V, Rodriguez Dominguez C, McAdam S. 2021. Linking xylem network failure with leaf tissue death. *New Phytologist* 232: 68–79.
- Brodrribb TJ, Bowman DJMS, Nichols S, Delzon S, Burtlett R. 2010. Xylem function and growth rate interact to determine recovery rates after exposure to extreme water deficit. *New Phytologist* 188: 533–542.
- Brodrribb TJ, Skelton RP, McAdam SAM, Bienaimé D, Lucani CJ, Marmottant P. 2016. Visual quantification of embolism reveals leaf vulnerability to hydraulic failure. *New Phytologist* 209: 1403–1409.
- Buckley RC, Corlett RT, Grubb PJ. 1980. Are the xeromorphic trees of tropical upper montane rain forests drought-resistant? *Biotropica* 12: 124.
- Burtlett R, Parise C, Capdeville G, Cochard H, Lamarque LJ, King A, Delzon S. 2022. Measuring xylem hydraulic vulnerability for long-vessel species: an improved methodology with the flow centrifugation technique. *Annals of Forest Science* 79: 5.
- Burnham KP, Anderson DR. 2010. *Model selection and multimodel inference: a practical information-theoretic approach*. New York, NY, USA: Springer.
- Campos H, Trejo C, Peña-Valdivia CB, García-Nava R, Conde-Martínez FV, Cruz-Ortega MR. 2014. Stomatal and non-stomatal limitations of bell pepper (*Capsicum annuum* L.) plants under water stress and re-watering: delayed restoration of photosynthesis during recovery. *Environmental and Experimental Botany* 98: 56–64.
- Carpenter B, Gelman A, Hoffman MD, Lee D, Goodrich B, Betancourt M, Brubaker M, Guo J, Li P, Riddell A. 2017. STAN: a probabilistic programming language. *Journal of Statistical Software* 76: 1.
- Duffy PB, Brando P, Asner GP, Field CB. 2015. Projections of future meteorological drought and wet periods in the Amazon. *Proceedings of the National Academy of Sciences, USA* 112: 13172–13177.
- Fan X-W, Li F-M, Song L, Xiong Y-C, An L, Jia Y, Fang X-W. 2009. Defense strategy of old and modern spring wheat varieties during soil drying. *Physiologia Plantarum* 136: 310–323.
- Fletcher LR, Scoffoni C, Farrell C, Buckley TN, Pellegrini M, Sack L. 2022. Testing the association of relative growth rate and adaptation to climate across natural ecotypes of *Arabidopsis*. *New Phytologist* 236: 413–432.
- Flynn DFB, Mirotchnick N, Jain M, Palmer MI, Naeem S. 2011. Functional and phylogenetic diversity as predictors of biodiversity–ecosystem-function relationships. *Ecology* 92: 1573–1581.
- Forner A, Aranda I, Granier A, Valladares F. 2014. Differential impact of the most extreme drought event over the last half century on growth and sap flow in two coexisting Mediterranean trees. *Plant Ecology* 215: 703–719.
- Galbraith D, Malhi Y, Affum-Baffoe K, Castanho ADA, Doughty CE, Fisher RA, Lewis SL, Peh KS-H, Phillips OL, Quesada CA *et al.* 2013. Residence times of woody biomass in tropical forests. *Plant Ecology & Diversity* 6: 139–157.
- Gould KS, Vogelmann TC, Han T, Clearwater MJ. 2002. Profiles of photosynthesis within red and green leaves of *Quintinia serrata*. *Physiologia Plantarum* 116: 127–133.
- Gourlet-Fleury S, Guehl J-M, Laroussinie O, ECOFOR (Group), eds. 2004. *Ecology and management of a Neotropical rainforest: lessons drawn from Paracou, a long-term experimental research site in French Guiana*. Paris, France: Elsevier.
- Granier A. 1987. Evaluation of transpiration in a Douglas-fir stand by means of sap flow measurements. *Tree Physiology* 3: 309–320.
- Guadagno CR, Ewers BE, Speckman HN, Aston TL, Huhn BJ, DeVore SB, Ladwig JT, Strawn RN, Weing C. 2017. Dead or alive? Using membrane failure and chlorophyll *a* fluorescence to predict plant mortality from drought. *Plant Physiology* 175: 223–234.
- Guan K, Pan M, Li H, Wolf A, Wu J, Medvigy D, Caylor KK, Sheffield J, Wood EF, Malhi Y *et al.* 2015. Photosynthetic seasonality of global tropical forests constrained by hydroclimate. *Nature Geoscience* 8: 284–289.
- Guan X-K, Song L, Wang T-C, Turner NC, Li F-M. 2015. Effect of drought on the gas exchange, chlorophyll fluorescence and yield of six different-era spring wheat cultivars. *Journal of Agronomy and Crop Science* 201: 253–266.
- Iqbal N, Hussain S, Raza MA, Yang C-Q, Safdar ME, Brestic M, Aziz A, Hayyat MS, Asghar MA, Wang XC *et al.* 2019. Drought tolerance of soybean (*Glycine max* L. Merr.) by improved photosynthetic characteristics and an efficient antioxidant enzyme activities under a split-root system. *Frontiers in Physiology* 10: 786.
- John GP, Henry C, Sack L. 2018. Leaf rehydration capacity: associations with other indices of drought tolerance and environment. *Plant, Cell & Environment* 41: 2638–2653.
- Johnson KM, Jordan GJ, Brodrribb TJ. 2018. Wheat leaves embolized by water stress do not recover function upon rewetting. *Plant, Cell & Environment* 41: 2704–2714.
- Kaiser WM. 1987. Effects of water deficit on photosynthetic capacity. *Physiologia Plantarum* 71: 142–149.
- Kannenberg SA, Novick KA, Alexander MR, Maxwell JT, Moore DJP, Phillips RP, Anderegg WRL. 2019. Linking drought legacy effects across scales: from leaves to tree rings to ecosystems. *Global Change Biology* 25: 2978–2992.
- Lamont BB, Lamont HC. 2000. Utilizable water in leaves of 8 arid species as derived from pressure–volume curves and chlorophyll fluorescence. *Physiologia Plantarum* 110: 64–71.
- Lee J-E, Frankenberg C, van der Tol C, Berry JA, Guanter L, Boyce CK, Fisher JB, Morrow E, Worden JR, Asefi S *et al.* 2013. Forest productivity and water stress in Amazonia: observations from GOSAT chlorophyll fluorescence. *Proceedings of the Royal Society B: Biological Sciences* 280: 20130171.
- Levionnois S, Ziegler C, Jansen S, Calvet E, Coste S, Stahl C, Salmon C, Delzon S, Guichard C, Heuret P. 2020. Vulnerability and hydraulic segmentations at the stem–leaf transition: coordination across Neotropical trees. *New Phytologist* 228: 512–524.

- Loubry D. 1994. La phénologie des arbres caducifoliés en forêt guyanaise (5° de latitude nord): illustration d'un déterminisme à composantes endogène et exogène. *Canadian Journal of Botany* 72: 1843–1857.
- Manzi OJL, Bellifa M, Ziegler C, Mihle L, Levionnois S, Burban B, Leroy C, Coste S, Stahl C. 2022. Drought stress recovery of hydraulic and photochemical processes in Neotropical tree saplings. *Tree Physiology* 42: 114–129.
- Maréchaux I, Bonal D, Bartlett MK, Burban B, Coste S, Courtois EA, Dulorme M, Goret J, Mira E, Mirabel A *et al.* 2018. Dry-season decline in tree sapflux is correlated with leaf turgor loss point in a tropical rainforest. *Functional Ecology* 32: 2285–2297.
- Maréchaux I, Saint-André L, Bartlett MK, Sack L, Chave J. 2020. Leaf drought tolerance cannot be inferred from classic leaf traits in a tropical rainforest. *Journal of Ecology* 108: 1030–1045.
- Miller G, Suzuki N, Ciftci-Yilmaz S, Mittler R. 2010. Reactive oxygen species homeostasis and signalling during drought and salinity stresses. *Plant, Cell & Environment* 33: 453–467.
- Molino J-F, Sabatier D. 2001. Tree diversity in tropical rain forests: a validation of the intermediate disturbance hypothesis. *Science* 294: 1702–1704.
- Moran JF, Becana M, Iturbe-Ormaetxe I, Frechilla S, Klucas RV, Aparicio-Tejo P. 1994. Drought induces oxidative stress in pea plants. *Planta* 194: 346–352.
- Munné-Bosch S, Jubany-Marí T, Alegre L. 2001. Drought-induced senescence is characterized by a loss of antioxidant defences in chloroplasts. *Plant, Cell & Environment* 24: 1319–1327.
- Murphy L. 2015. *LIKELIHOOD: methods for maximum likelihood estimation* [WWW document] URL <https://cran.r-project.org/web/packages/likelihood/index.html> [accessed 15 May 2023].
- Oppenheimer HR, Leshem B. 1966. Critical thresholds of dehydration in leaves of *Nerium oleander* L. *Protoplasma* 61: 302–321.
- Pineda-García F, Paz H, Meinzer FC. 2012. Drought resistance in early and late secondary successional species from a tropical dry forest: the interplay between xylem resistance to embolism, sapwood water storage and leaf shedding. *Plant, Cell & Environment* 36: 405–418.
- Ploughe LW, Jacobs EM, Frank GS, Greenler SM, Smith MD, Dukes JS. 2019. Community Response to Extreme Drought (CRED): a framework for drought-induced shifts in plant–plant interactions. *New Phytologist* 222: 52–69.
- Saglam A, Saruhan N, Terzi R, Kadioglu A. 2011. The relations between antioxidant enzymes and chlorophyll fluorescence parameters in common bean cultivars differing in sensitivity to drought stress. *Russian Journal of Plant Physiology* 58: 60–68.
- Sancho-Knapik D, Álvarez-Arenas TG, Peguero-Pina JJ, Fernández V, Gil-Pelegrín E. 2011. Relationship between ultrasonic properties and structural changes in the mesophyll during leaf dehydration. *Journal of Experimental Botany* 62: 3637–3645.
- Saveyn A, Steppe K, Lemeur R. 2007. Drought and the diurnal patterns of stem CO₂ efflux and xylem CO₂ concentration in young oak (*Quercus robur*). *Tree Physiology* 27: 365–374.
- Silva EN, Silveira JAG, Ribeiro RV, Vieira SA. 2015. Photoprotective function of energy dissipation by thermal processes and photorespiratory mechanisms in *Jatropha curcas* plants during different intensities of drought and after recovery. *Environmental and Experimental Botany* 110: 36–45.
- Skelton RP, Brodrribb TJ, McAdam SAM, Mitchell PJ. 2017. Gas exchange recovery following natural drought is rapid unless limited by loss of leaf hydraulic conductance: evidence from an evergreen woodland. *New Phytologist* 215: 1399–1412.
- Song Y, Sterck F, Zhou X, Liu Q, Kruijt B, Poorter L. 2022. Drought resilience of conifer species is driven by leaf lifespan but not by hydraulic traits. *New Phytologist* 235: 978–992.
- Souza RP, Machado EC, Silva JAB, Lagôa AMMA, Silveira JAG. 2004. Photosynthetic gas exchange, chlorophyll fluorescence and some associated metabolic changes in cowpea (*Vigna unguiculata*) during water stress and recovery. *Environmental and Experimental Botany* 51: 45–56.
- Stahl C, Burban B, Bompy F, Jolin ZB, Sermage J, Bonal D. 2010. Seasonal variation in atmospheric relative humidity contributes to explaining seasonal variation in trunk circumference of tropical rain-forest trees in French Guiana. *Journal of Tropical Ecology* 26: 393–405.
- Stahl C, Burban B, Wagner F, Goret J-Y, Bompy F, Bonal D. 2013. Influence of seasonal variations in soil water availability on gas exchange of tropical canopy trees. *Biotropica* 45: 155–164.
- Stan Development Team. 2018. *RSTAN: the R interface to STAN*. R package v.2.21.8. [WWW document] URL <https://mc-stan.org/> [accessed 15 May 2023].
- Sterck F, Markesteijn L, Schieving F, Poorter L. 2011. Functional traits determine trade-offs and niches in a tropical forest community. *Proceedings of the National Academy of Sciences, USA* 108: 20627–20632.
- Trifilò P, Petruzzellis F, Abate E, Nardini A. 2021. The extra-vascular water pathway regulates dynamic leaf hydraulic decline and recovery in *Populus nigra*. *Physiologia Plantarum* 172: 29–40.
- Trueba S, Pan R, Scoffoni C, John GP, Davis SD, Sack L. 2019. Thresholds for leaf damage due to dehydration: declines of hydraulic function, stomatal conductance and cellular integrity precede those for photochemistry. *New Phytologist* 223: 134–149.
- Trugman AT, Detto M, Bartlett MK, Medvigy D, Anderegg WRL, Schwalm C, Schaffer B, Pacala SW. 2018. Tree carbon allocation explains forest drought-kill and recovery patterns. *Ecology Letters* 21: 1552–1560.
- Vollenweider P, Menard T, Arend M, Kuster TM, Günthardt-Goerg MS. 2016. Structural changes associated with drought stress symptoms in foliage of Central European oaks. *Trees* 30: 883–900.
- Wagner F, Héroult B, Stahl C, Bonal D, Rossi V. 2011. Modeling water availability for trees in tropical forests. *Agricultural and Forest Meteorology* 151: 1202–1213.
- Wagner F, Rossi V, Stahl C, Bonal D, Héroult B. 2012. Water availability is the main climate driver of Neotropical tree growth. *PLoS ONE* 7: e34074.
- Wagner F, Rossi V, Stahl C, Bonal D, Héroult B. 2013. Asynchronism in leaf and wood production in tropical forests: a study combining satellite and ground-based measurements. *Biogeosciences* 10: 7307–7321.
- Xiong D, Nadal M. 2020. Linking water relations and hydraulics with photosynthesis. *The Plant Journal* 101: 800–815.
- Yang H, Ciais P, Wang Y, Huang Y, Wigneron J, Bastos A, Chave J, Chang J, Doughty C, Fan L *et al.* 2021. Variations of carbon allocation and turnover time across tropical forests. *Global Ecology and Biogeography* 30: 1271–1285.
- Yang Y, Saatchi SS, Xu L, Yu Y, Choi S, Phillips N, Kennedy R, Keller M, Knyazikhin Y, Myneni RB. 2018. Post-drought decline of the Amazon carbon sink. *Nature Communications* 9: 3172.
- Yuan W, Zheng Y, Piao S, Ciais P, Lombardozzi D, Wang Y, Ryu Y, Chen G, Dong W, Hu Z *et al.* 2019. Increased atmospheric vapor pressure deficit reduces global vegetation growth. *Science Advances* 5: eaax1396.
- Zhang F-J, Zhang K-K, Du C-Z, Li J, Xing Y-X, Yang L-T, Li Y-R. 2015. Effect of drought stress on anatomical structure and chloroplast ultrastructure in leaves of sugarcane. *Sugar Tech* 17: 41–48.
- Zhu S-D, Chen Y-J, Ye Q, He P-C, Liu H, Li R-H, Fu P-L, Jiang G-F, Cao K-F. 2018. Leaf turgor loss point is correlated with drought tolerance and leaf carbon economics traits. *Tree Physiology* 38: 658–663.
- Ziegler C, Coste S, Stahl C, Delzon S, Levionnois S, Cazal J, Cochard H, Esquivel-Muelbert A, Goret J-Y, Heuret P *et al.* 2019. Large hydraulic safety margins protect Neotropical canopy rainforest tree species against hydraulic failure during drought. *Annals of Forest Science* 76: 115.
- Zwieniecki MA, Brodrribb TJ, Holbrook NM. 2007. Hydraulic design of leaves: insights from rehydration kinetics. *Plant, Cell & Environment* 30: 910–921.

Supporting Information

Additional Supporting Information may be found online in the Supporting Information section at the end of the article.

Fig. S1 Relationships between the relative water content of the dehydrated leaves (RWC_d) and percent loss of rehydration capacity (PLRC) for the eight focal species.

Fig. S2 Relationships between RWC_d and the percent loss of photochemical function (PLCF) for the eight focal species.

Fig. S3 Sensitivity analysis demonstrating a negligible effect of seasonal osmotic adjustment on estimates for the water potential thresholds for persistent leaf damage.

Fig. S4 Relationships between safety margins for persistent damage and embolism and drought resilience in stem diameter growth rates.

Methods S1 Supplementary methods.

Table S1 Dataset used to calculate PLRC, PLCF, and the thresholds for persistent damage to rehydration capacity and chlorophyll fluorescence.

Table S2 Best-fit models relating the relative water content of the dehydrated leaves (RWC_d) to PLRC and PLCF.

Table S3 Trait dataset for the eight focal species.

Table S4 Uncertainty estimates for the RWC thresholds for persistent damage.

Table S5 Safety margins for incipient (12%) embolism for the trees measured for sapflow resilience to drought.

Table S6 Safety margins for persistent damage and embolism for the species measured for growth resilience to drought.

Table S7 Fitted parameter values for the growth resilience models.

Please note: Wiley is not responsible for the content or functionality of any Supporting Information supplied by the authors. Any queries (other than missing material) should be directed to the *New Phytologist* Central Office.